IOP Publishing Nanotechnology
Nanotechnology 28 (2017) 165502 (10pp) https://doi.org/10.1088/1361-6528/aa6320

Synthesis of novel nitrogen-doped carbon dots for highly selective detection of iron ion

Pengfei Lv, Yixin Yao, Huimin Zhou, Jin Zhang, Zengyuan Pang, Kelong Ao, Yibing Cai and Qufu Wei[1]

Key Laboratory of Eco-textiles, Jiangnan University, Wuxi 214122, People's Republic of China

E-mail: 18861800875@163.com, 18801510310@163.com, xjzhouhuimin@126.com, 7160707010@vip.jiangnan.edu.cn, pangzengyuan1212@163.com, aokelong_jnu@126.com, yibingcai@163.com and qfwei@jiangnan.edu.cn

Received 15 January 2017, revised 14 February 2017
Accepted for publication 27 February 2017
Published 22 March 2017

Abstract

Herein, we report an eco-friendly and simple fluorescent nitrogen-doped carbon quantum dot (N-CQD) biosensor which was synthesized via a hydrothermal method using erhanediamine (EDA) and citric acid (CA) as precursors. The surface functionalization of N-CQDs exhibited a bright blue emission under the excitation wavelength of 350 nm. The obtained N-CQDs were characterized by atomic force microscopy (AFM), Fourier transform infrared spectroscopy, x-ray photoelectron spectroscopy, and transmission electron microscopy. It was found that the surface of the CQDs was successfully functionalized. After that, as-prepared N-CQDs were further applied in Fe(III) detection. Spectroscopic data indicated that fluorescent carbon-based nanomaterials displayed a sensitive response to Fe^{3+} in the range of 0.5–1000 μM as a fluorescence sensor in real environmental samples. Furthermore, the results also showed that a novel N-CQD nanomaterial could be employed as an ideal fluorescent Fe(III) probe.

Keywords: carbon quantum dots, fluorescence, sensor, Fe(III), detection

(Some figures may appear in colour only in the online journal)

Introduction

In recent years, the study of Fe(III) ion (Fe^{3+}) has attracted considerable attention. It is well known that Fe metal ions plays a vital role in the life system; excess Fe will cause cell oxidation and the annihilation of blood circulation in the human body (Lin *et al* 2009). Exploiting the rapid, precise, and highly-efficient detection methods for heavy metal ions has attracted worldwide attention (Zuo *et al* 2016). Fluorescent carbon-based nanomaterials, with unique properties and special small-sized effect, have become the research focus. As previous studies revealed, spectrophotometry, atomic adsorption spectrometry, and inductively coupled plasma mass spectrometry can be applied in Fe^{3+} analysis. However, these traditional methods have their drawbacks, mainly including poor selectivity, fixed cumbersome instruments, complicated analysis procedure, and so forth. To date, many kinds of as-prepared carbon-based fluorescent materials have been studied, such as fluorescent graphene oxide (GO) (Tan *et al* 2016, Zhang *et al* 2016), polymer dots (PDs) (Wang *et al* 2016), carbon nanotubes (Welsher *et al* 2009), graphene quantum dots (GQDs) (Ponomarenko *et al* 2008, Konstantatos *et al* 2012, Sheng *et al* 2014, Yoon *et al* 2016), etc. Fluorescent probes containing fluorescent nanoparticles, as an advanced versatile nanomaterial, have been widely used for technical applications, such as electrocatalysis, photocatalysis, photodynamic therapy, drug delivery, bioimaging, biosensing, and chemical sensing (Lim *et al* 2015). These can also react with Fe^{3+}, leading to the transformation of fluorescent intensity, which can be utilized to design fluorescent probes. Over the years, these fluorescent probes of semiconductor QDs have been commonly used due to their tunable and strong fluorescence emission properties for wide practical application, including bioimaging and biosensing. Nevertheless, it is known that metal semiconductor materials are highly poisonous and relatively expensive. Thus, the exploitation of facile synthesis and low-cost alternative materials have attracted extensive interest in recent years. As

[1] Author to whom any correspondence should be addressed.

reported by Xu *et al* (Xu *et al* 2004), carbon quantum dots (CQDs) were accidentally discovered due to the separation and purification of single-walled carbon nanotubes. In recent years, CQDs have been exploited using two routes, namely the bottom-up route (Liu *et al* 2009, Zhu *et al* 2015) and top-down route (Fernando *et al* 2015, Zheng *et al* 2015). As a novel kind of fluorescent material, compared to traditional semiconductor QDs, CQDs possess fluorescent properties similar to other semiconductor QDs and simultaneously possess many advantages such as favorable biocompatibility, chemical stability, water solubility, tunable surface functionalities, and low toxicity (Zhao *et al* 2011, Wu *et al* 2013). Depending on these qualities, CQDs have been widely applied in many areas such as nanomedicine, bioimaging, catalysis, photovoltaic devices, and biosensors. When CQDs are combined with Fe^{3+}, these two materials form a sort of complex and the fluorescence intensity of CQDs will decline, which is referred to as the 'turn-off' phenomenon, attributed to the quenching behavior of CQDs. Based on this characteristic of CQDs, a variety of fluorescent sensors for the detection of Fe^{3+} using CQDs have been studied. A simple and efficient hydrothermal treatment of garlic, to synthesize novel fluorescent nitrogen and sulfur co-doped carbon dots (N,S,C-CQDs) for the detection of Fe^{3+} was described by Chen and co-authors (Chen *et al* 2015). Yang and co-authors reported an innovative and eco-friendly method to synthesize CQDs originated from honey, and the obtained CQDs were used to detect Fe^{3+} with a linear range of 5.0×10^{-9}–1.0×10^{-4} mol l^{-1} and a low detection limit range of 1.7×10^{-9} mol l^{-1} (Yang *et al* 2014). Fong and co-authors reported a facile pyrolytic synthesis of CQDs from sodium alginate, which was further applied for Fe^{3+} detection (Fong *et al* 2016).

In this paper, we developed a simple, green fluorescence probe via the hydrothermal method using ethanediamine (EDA) and citric acid (CA) as precursors. The morphology, structure, and properties of the as-prepared nitrogen-doped carbon quantum dots (N-CQDs) were investigated. Besides, the as-prepared N-CQD nanomaterials were utilized as a fluorescent probe for the detection of Fe^{3+} in water environment by analyzing the change of the fluorescence intensity of the sample. The satisfactory fluorescence analysis results showed that the obtained N-CQDs are good materials for the fluorescent probe of heavy metal ions.

Experimental

Reagents

CA and EDA were purchased from Shanghai Aladdin Bio-Chem Technology Co., Ltd (Shanghai, China). The solutions of 5 mM of NaCl, KCl, $MgSO_4$, $CoCl_2$, $CaCl_2$, $NiCl_2$, $CuCl_2$, $CdCl_2$, LiCl, $FeCl_3$, $PbCl_2$, $FeCl_2$, Al_2Cl_3, $Cr(NO_3)_3$, $AgNO_3$, $MnCl_2$, $SnCl_2$, $Zn(NO_3)_2$ were obtained from Sinopharm Chemical Reagent Co., Ltd (China). All of the chemicals were of analytical grade and the solutions were achieved with ultrapure water.

Synthesis of fluorescent N-CQDs

The details of the synthesis procedure are described as follows: 0.1 ml EDA and 1.8 g CA were dispersed into 60 ml ultrapure water in a 100 ml beaker by stirring for 30 min to ensure uniform dispersion. Then, the mixture was transferred into a 100 ml Teflon-lined autoclave and heated for 5 h at 220 °C by a hydrothermal method. The precipitate was centrifuged at 4000 rpm for 5 min, then repeated three times to obtain the pale yellow supernatant. Subsequently, the supernatant was dispersed in a dialysis bag (retained molecular weight: 1000 Da) for 24 h to remove small molecules. Eventually, blue fluorescent N-CQDs were further concentrated up to10 mg ml^{-1} in deionized water.

Measurement and characterization

The Fourier transform infrared (FT-IR) spectra of the N-CQDs were recorded by FT-IR (Nicolet Nexus, Thermo Electron Corporation, Waltham, MA, USA) over the wavenumber ranging from 400–4000 cm^{-1}. Topography images of the N-CQDs were characterized by atomic force microscopy (AFM) (CSPM 4000, Benyuan, China) in tapping mode at room temperature in atmosphere, and samples were obtained by dropping the solution onto the substrate of mica. X-ray photoelectron spectroscopy (XPS) was obtained by a Thermo Scientific Escalab 250Xi (Thermo Fisher Scientific, Waltham, MA, USA) with monochromatized Al Ka radiation. The morphology and average diameter of the resultant as-prepared N-CQDs were obtained by high-resolution transmission electron microscopy (HR-TEM) using a JEM-2100 (Tokyo, Japan) operating at an accelerating voltage of 200 kV, and the N-CQD solution was placed over a copper mesh support and dried under ambient conditions. The UV–vis spectra were obtained with a U-3000 spectrophotometer (Hitachi, Japan). Fluorescence measurements were performed using an Hitachi F-7000 spectrometer (Tokyo, Japan) with an excitation wavelength of 350 nm.

Response to different metal ions

To further study the sensing ability of the as-prepared N-CQDs to different metal ions, all samples were subsequently dissolved in ultrapure water (100 ml) to afford 1 mM in aqueous solutions by stirring for 10 min till uniformly dispersed. All the as-prepared samples were added into the N-CQDs and then the fluorescence spectra data of all samples were recorded under the excitation at 350 nm. Then, the solvent from the deionized water was replaced by real lake water. The performance of the N-CQDs for real sample analysis was studied under the excitation at 350 nm.

Results and discussion

Morphology and surface study

It can be clearly seen that the well-dispersed quantum dots were synthesized by using a hydrothermal method, as shown

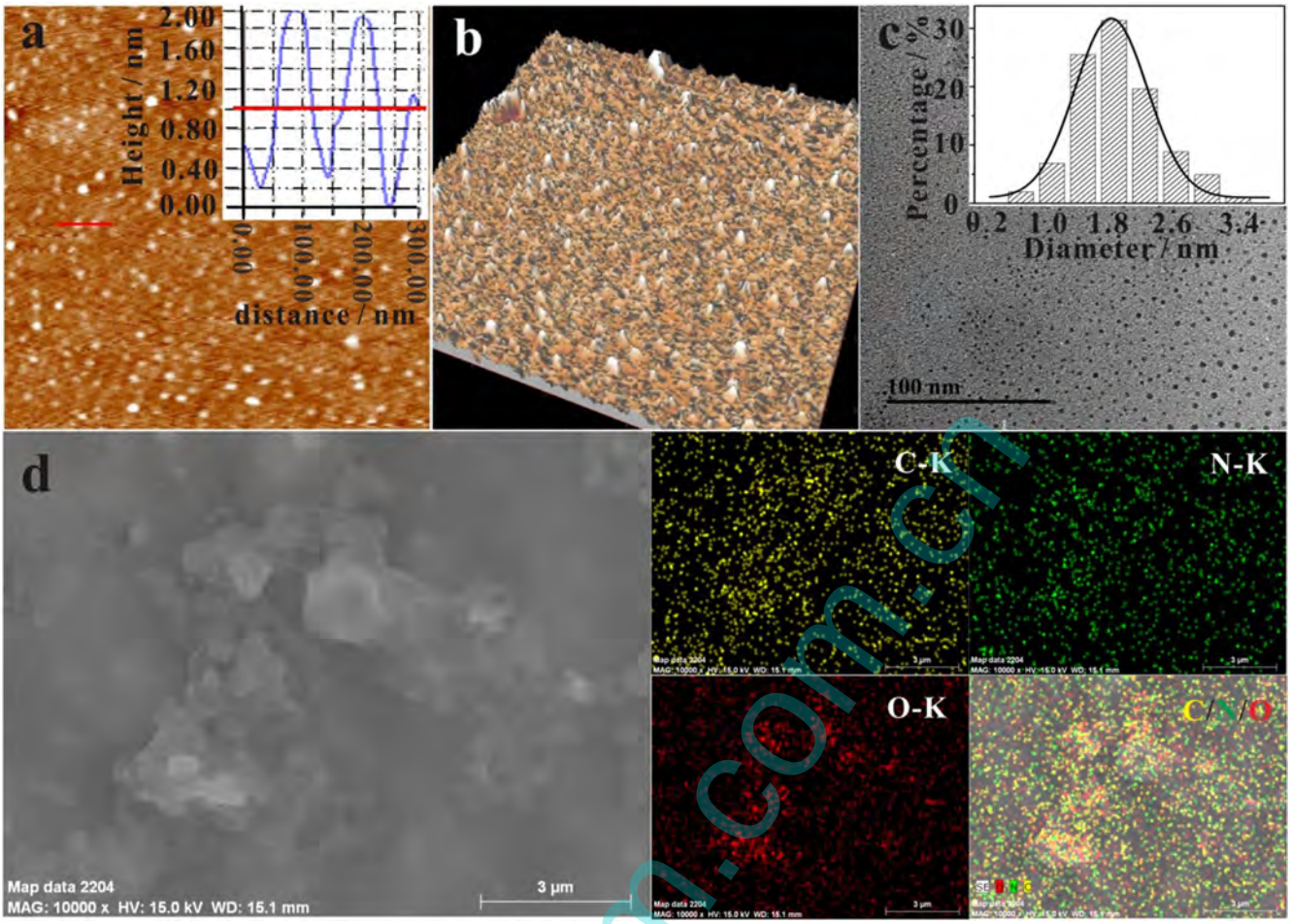

Figure 1. (a), (b) AFM images of the synthesized N-CQDs (Top Right: the height profile and average size of the N-CQDs); (c) TEM image of the synthesized N-CQDs, inset showing particle size distribution of the synthesized N-CQDs; (d) Element mapping of the N-CQDs: typical HAADF-STEM image of the N-CQDs (including C, N, and O elemental mapping of the N-CQDs).

in figure 1(a). The height profiles display that the typical topographic height difference of the N-CQDs approached 2 nm, as illustrated in figure 1(a). Figure 1(b) reveals the small spherical morphology of the N-CQDs. As is evident from the as-prepared N-CQDs in figure 1(c), the TEM image displays the stable dispersions of the N-CQDs in aqueous solution, while concomitantly their diameters were mainly distributed in the range of 0.6–3.4 nm with an average diameter of about 1.8 nm. Figure 1(d) presents the high angle annular dark field (HAADF) scanning transmission electron microscopy (STEM) images and the elemental mapping of the synthesized N-CQDs, which revealed the presence of C, N, and O in the synthesized N-CQDs. To evaluate the chemical composition of C, N, and O, the change of surface chemical bonding was further verified, as shown in figure 2.

Structural information of the synthesized N-CQDs was further studied by FT-IR, as shown in figure 2(A). Figure 2(A) indicates that the as-prepared N-CQDs possessed rich nitrogen/oxygen-containing groups including carboxyl, hydroxyl, and amino groups (Xu *et al* 2015, Lu *et al* 2016), as the following were observed: stretching vibrations of C=O at 1730 cm^{-1}, bending vibrations of N-H at 1641 cm^{-1}, stretching vibrations of C-N at 1307 cm^{-1}, stretching vibrations of C-O at 1164 cm^{-1}, and asymmetric stretching vibrations of C-NH-C at 1112 cm^{-1} (Yu 2015, Han *et al* 2016). Moreover, the peaks around 3402 cm^{-1} correspond to the absorption features of the stretching vibrations of the O-H and N-H groups (Zhang and Chen 2014), and the peaks at 2905 cm^{-1} were attributed to the C-H bond stretching vibrations (Zhou *et al* 2015).

To further analyze the structural information of N-CQDs, XPS was performed. The XPS full scan spectrum of N-CQDs, as shown in figure 2(B), indicates two predominant peaks at 532 and 285 eV and a weak peak at 400 eV, corresponding to the binding energies of O1s, C1s, and N1s, respectively (Niu *et al* 2015). The content of the three elements of the N-CQDs was presented as follows: 18.06% (O), 8.27% (N), and 73.67% (C), respectively, as illustrated in figure 2(B) Meanwhile, the high-resolution spectrum of C1s further confirms that the presence of four peaks at 287.8, 286.5, 285.4 and 284.3 eV, which were attributed to C=O, C-O, C-N and C-C (sp^3) bonds, respectively (Yu *et al* 2015, Atchudan *et al* 2016), as described in figure 2(C). Figure 2(D) displays the one major peak that occurred around 399.5 eV, corresponding to N-C (H_2N-C) bonds on the surface of the N-CQDs (Gong *et al* 2014). FT-IR and XPS results confirmed that the

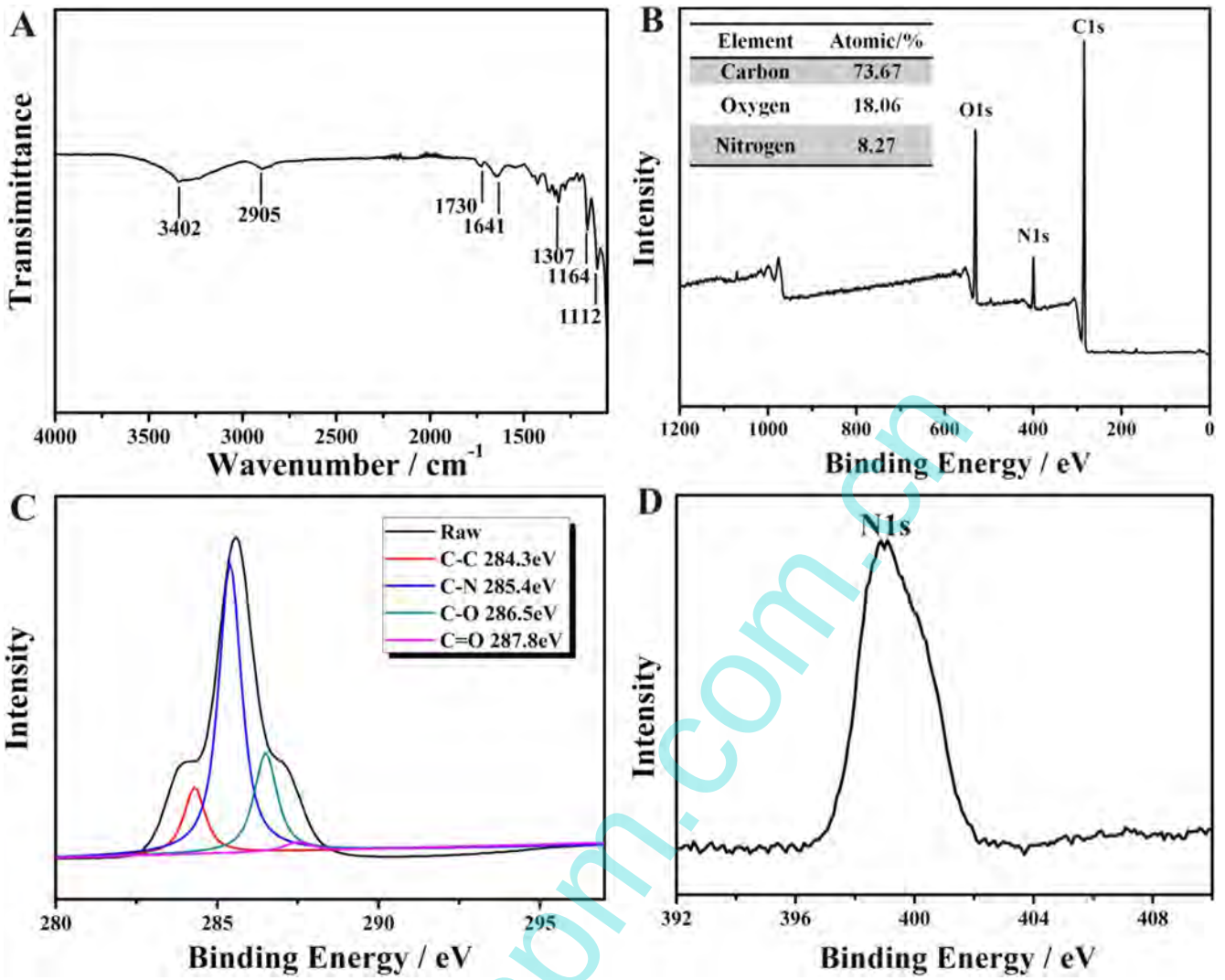

Figure 2. (A) FT-IR spectra of the N-CQDs; (B) XPS survey spectrum and element content of the N-CQDs; (C), (D) high-resolution XPS spectra of C1s and N1s, respectively.

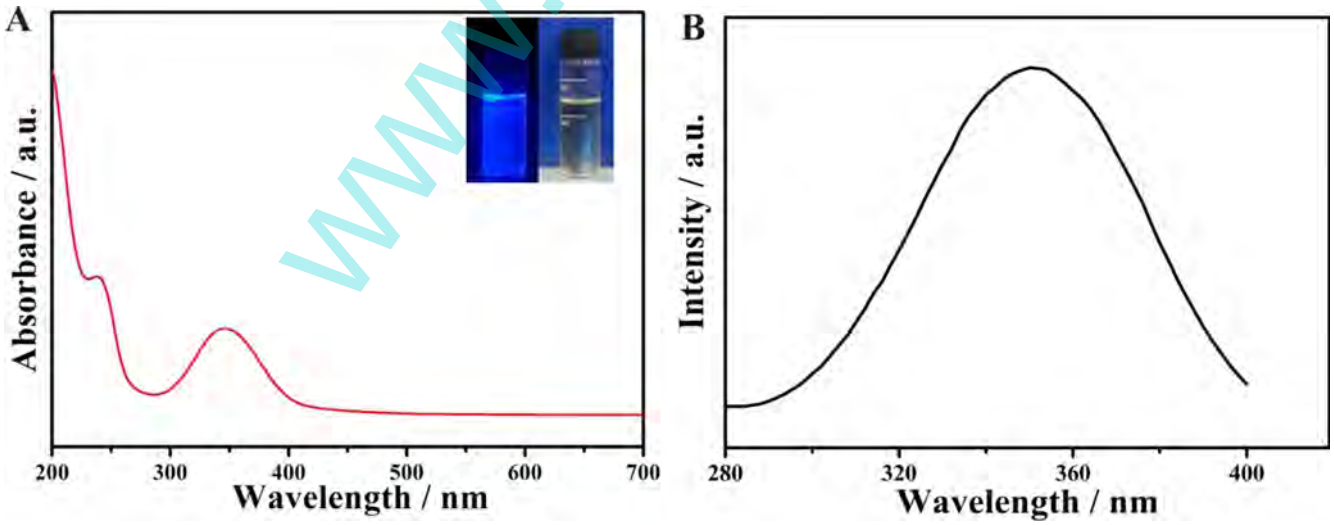

Figure 3. (A), (B) UV–vis absorption and the fluorescence spectra of the sample: insets in (A) show the photographs under visible light (right) and UV light (left) of 350 nm.

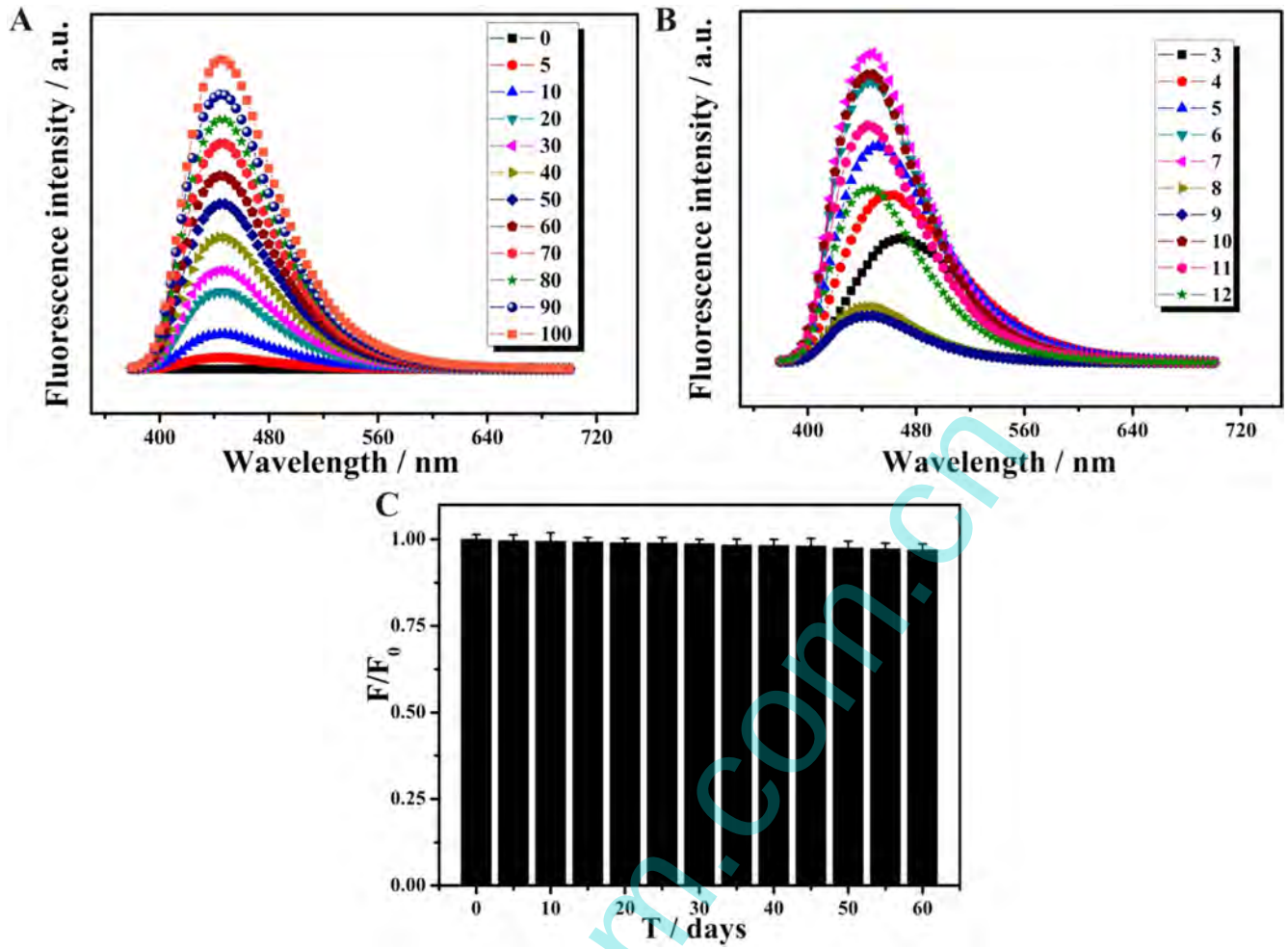

Figure 4. (A) Fluorescence emission spectra with the concentration increments of N-CQDs (μg/ml): from 0 to100 in deionized water; (B) Fluorescence intensity change of N-CQDs at different pH (pH 3–12 from down to up) under UV light of 350 nm. (C) Effect of time on the fluorescence intensity of the N-CQDs (0–60 days).

N-CQDs were functionalized by nitrous ($-NH_2$), hydroxyl ($-OH$), and ($-C{=}O$) groups.

Optical property analysis

UV–vis absorption measurement is a simple method applicable to the analysis of the structural changes of a compound. Hence, the optical properties of the as-prepared N-CQDs were analyzed by UV–vis spectroscopy. UV–vis absorption and fluorescence excitation spectra of the sample in water solution are shown in figures 3(A) and (B), which indicate a predominant absorption band located at 350 nm and a weak absorption band located at 240 nm, attributed to the n-π^* transition of C=O and π-π^* transition of carbon core, respectively (Li *et al* 2015a, Edison *et al* 2016). Meanwhile, the N-CQDs displayed as transparent yellow under visible light, while concomitantly appearing as a strong bright blue color under UV light at 350 nm, as shown in the inset photograph of figure 3(A). In order to investigate the effect of different conditions on fluorescent properties of the N-CQDs, as-prepared N-CQDs were further analyzed by using an Hitachi F-7000 spectrometer, as illustrated in figure 4.

Figure 4 reveals the relation of the fluorescent intensity of N-CQDs with different N-CQD concentration between 0 μg ml^{-1} and 100 μg ml^{-1}. Significant increases in emission intensity were recorded with the increase of the concentration, attributed to the quantum dot increase. A series of samples with pH ranging systematically from 3–11 were prepared, while concomitantly the fluorescence intensity of the fluorescent N-CQDs at different values of pH was observed. Figure 4(B) obviously indicates dramatic changes in emission intensity as the pH was varied. The fluorescent intensity of N-CQDs prominently changed with the pH increases from 3.5 to 7, reaching an optimum value around pH = 7, but it decreased from 7 to 12, which might be attributed to non-covalent molecular interactions of N-CQDs, as depicted in figure 4(B). In summary, the photoluminescence (PL) was found to be strongly dependent as the pH varied under UV light of 350 nm. The effect of time on the fluorescent intensity of the N-CQDs was also further confirmed and the results are recorded in figure 4(C). The fluorescent intensity of the as-prepared sample exhibited remarkable stability, with almost no change observed with the passage of time. The residual fluorescent intensity of the N-CQDs retained about 96.9% of

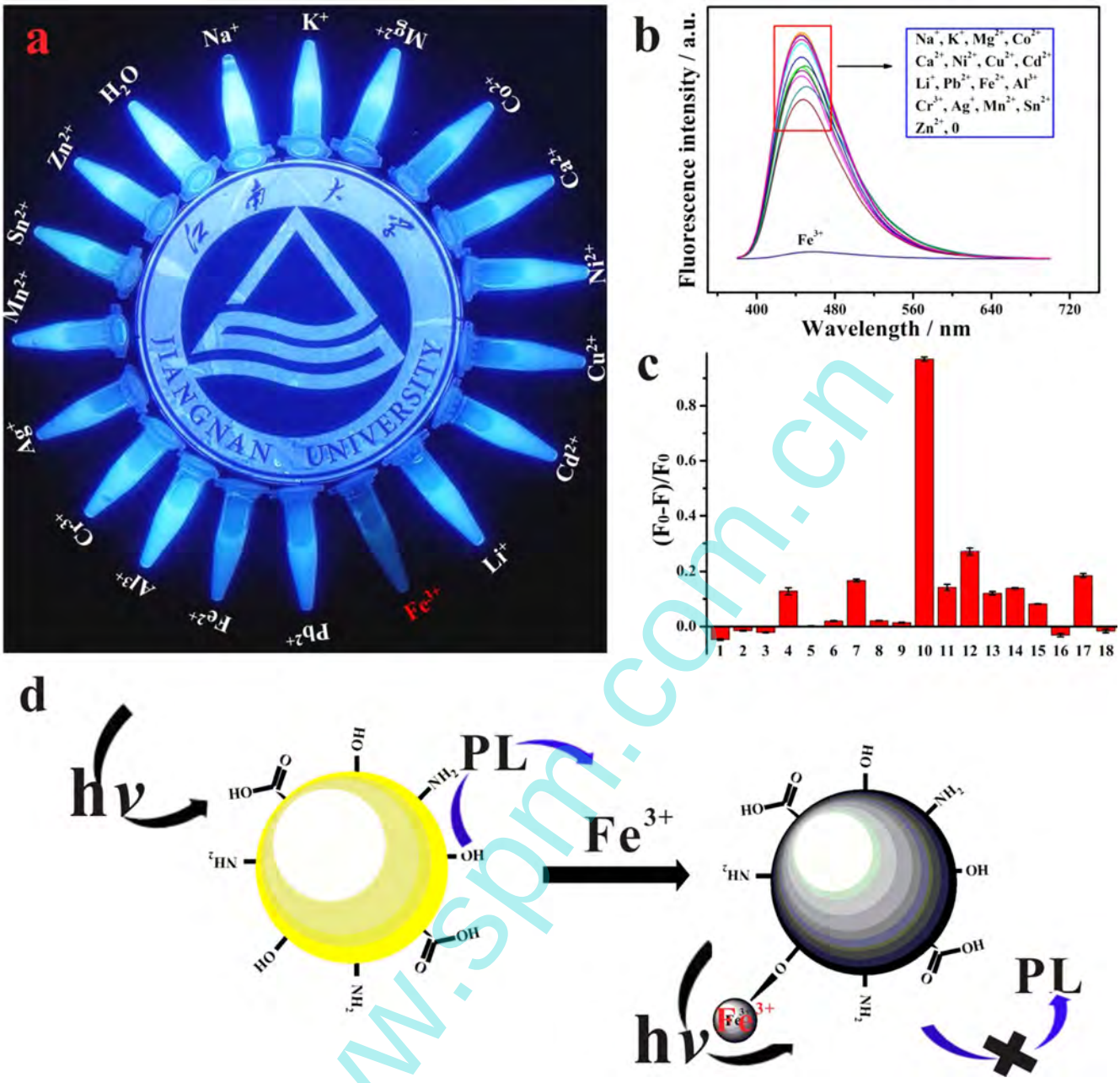

Figure 5. (a) Fluorescence schematic of N-CQDs with different metal ions (under UV light of 350 nm); (b) Fluorescence spectra of N-CQDs after adding 1 mM of metal salts in water solutions; (c) The different $(F_0\text{-}F)/F_0$ values (fluorescence intensity ratio) of the N-CQD solutions upon the condition of existing individual metal ions: Na^+, K^+, Mg^{2+}, Co^{2+}, Ca^{2+}, Ni^{2+}, Cu^{2+}, Cd^{2+}, Li^+, Fe^{3+}, Pb^{2+}, Fe^{2+}, Al^{3+}, Cr^{3+}, Ag^+, Mn^{2+}, Sn^{2+}, Zn^{2+}, H_2O; (d) The schematic mechanism of the fluorescence quenching of N-CQDs to Fe^{3+} ions.

their original value after 60 days. In general, as-prepared N-CQDs are considered to be comparatively stable fluorescent detection nanomaterials.

In order to investigate the sensing ability of the as-prepared N-CQDs to different metal ions, representative metal ion solutions were subsequently prepared, stirring them for 10 min till uniformly dissolved, including Na^+, K^+, Mg^{2+}, Co^{2+}, Ca^{2+}, Ni^{2+}, Cu^{2+}, Cd^{2+}, Li^+, Fe^{3+}, Pb^{2+}, Fe^{2+}, Al^{3+}, Cr^{3+}, Ag^+, Mn^{2+}, Sn^{2+}, Zn^{2+} (1 mM). All the as-prepared samples were added into the N-CQDs and then the fluorescence properties of the samples were measured under excitation at 350 nm by an Hitachi F-7000 spectrometer, as displayed in figure 5(a). Figure 5(a) reveals a quenched PL response to Fe(III) ion. In contrast, the addition of other metal ions had no obvious quenching effect that can be detected by the naked eye, and all the samples displayed a blue color, which implied that the as-prepared N-CQD-based fluorescent materials possessed high selectivity to Fe(III) and can be better applied in sensors for metal detection. The variation of fluorescence intensity of the N-CQDs after adding different metal ions was further tested, as described in figure 5(b). The data show that the fluorescence intensity of the N-CQDs to Fe(III) ion approached constant (0). Figure 5(b) further verifies this finding that the N-CQDs displayed high selectivity to

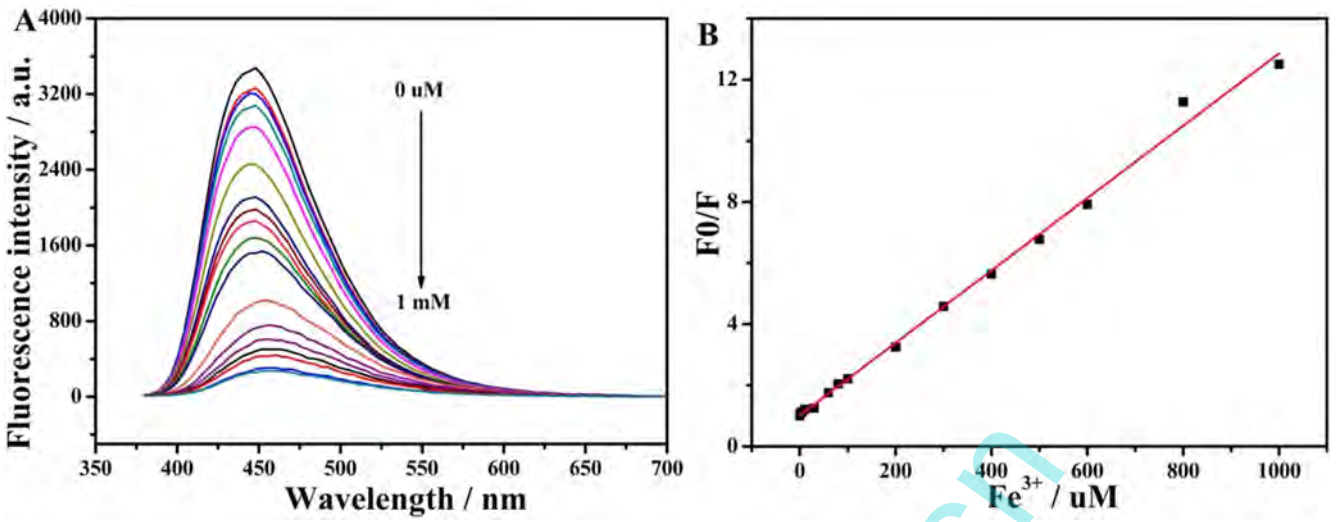

Figure 6. (A) Fluorescence spectra of the N-CDs in the presence of various concentrations of Fe^{3+} (From top to bottom: 0–1000 μM); (B) Linear relationship between the F0/F and Fe^{3+} concentration.

Fe(III) ion, because Fe^{3+} ions exhibit a higher affinity for O and N on the N-CQD surface, and facilitate aggregation to forming N-CQDs-Fe^{3+} chelate, causing fluorescence quenching (Lai *et al* 2013, Qian *et al* 2014, Iqbal *et al* 2016). Meanwhile, as indicated in figure 5(c), the fluorescence changing ratio (F_0-F)/F is immediately described, in which F_0 and F are defined as the fluorescence intensities of the as-prepared N-CQDs at 350 nm in the absence and presence of metal ions, respectively. The data clearly showed the ratio (F_0-F)/F of added Fe(III) ion was close to constant (1), implying a quenched PL response to Fe(III) ion.

According to previous literature reported (Qu *et al* 2013, Zhang *et al* 2014), the fluorescence quenching mechanism of carbon-based quantum dots interact with Fe^{3+}, as displayed in figure 5(d). The added Fe(III) ions coordinate with phenolic hydroxyl groups (−OH) on the N-CQD surface, resulting in the formation of a stable Fe(III)-complex chelate (Mei *et al* 2012). After that, the electrons in the excited state of the N-CQDs are transferred to the half-filled 3d orbitals of Fe^{3+}, thus facilitating the non-radiative electron–hole recombination and causing significant fluorescence quenching (Jiang *et al* 2015), as follows in equation (1):

$$6CQD - OH + Fe^{3+} \rightarrow [Fe(OCQD)_6]^{3+} + 6H^{+}. \quad (1)$$

To evaluate the sensitivity of the as-prepared fluorescent N-CQD nanomaterial, the fluorescence intensity spectra of the obtained N-CQDs with different concentrations of Fe(III) were obtained using fluorescence titrations after 10 min of incubation, as shown in figure 6(A). The fluorescence intensity of the as-prepared N-CQDs at 350 nm was gradually quenched with the increase of Fe(III) ion concentration (0–1000 μM). As shown in figure 6(B), a good linear relationship between the fluorescence intensity ratio (F0/F) and Fe(III) ion concentration in the range of 0–1000 μM is observed. The corresponding regression coefficient (R^2) between different concentrations of Fe(III) ions and the fluorescence intensity is 0.995 (n = 4). These results indicated that the as-prepared N-CQDs could be promising for Fe(III) ion detection in aqueous media. Meanwhile, the quenching efficiency of the Fe(III) ions was defined as the following correlation equation (2):

$$F_0/F = 1.02012 + 0.01184{*}C_{Fe}^{3+} \quad (2)$$

where F and F_0 are the fluorescence intensity of the obtained N-CQDs in the presence and absence of Fe(III) ion, respectively. The detection limit (LOD) to Fe^{3+} was calculated by employing the following equation (3):

$$LOD = \frac{3\sigma}{K} \quad (3)$$

where σ and K are defined as the standard deviation of (F0/F) values and K represents the slope of the linear line, respectively. The LOD of Fe^{3+} was estimated to be 79 nM at a signal-to-noise ratio of 3. Overall, the results revealed a relatively higher sensitive to Fe^{3+}.

Table 1. List of fluorescent carbon-based QDs for Fe^{3+} detection.

Fluorescent probes	Linear range (μM)	Detection limit (μM)	Ref
N-GQDs	1–1945	0.09	(Jian and Chen 2014)
S-CDs	0–500	0.1	(Xu *et al* 2014)
Co-CDs	$2^{*}10^{-3}$–3	0.22	(Chen *et al* 2015)
N, S-CDs	25–500	4	(Ding *et al* 2014)
NA-GQDs	0.5–500	0.1	(Li *et al* 2015b)
GO	5–50	0.64	(Mei *et al* 2012)
N-CQDs	0.5–1000	0.079	this work

Compared to different carbon-based fluorescent nanomaterials to Fe^{3+} detection reported in the literature, the linear ranges and detection limits of the as-prepared N-CDs are also displayed, as described in table 1. It can be seen that the obtained fluorescent carbon-based nanomaterials endowed themselves satisfactory detection properties to Fe^{3+}. In summary, carbon-based fluorescent materials could be a

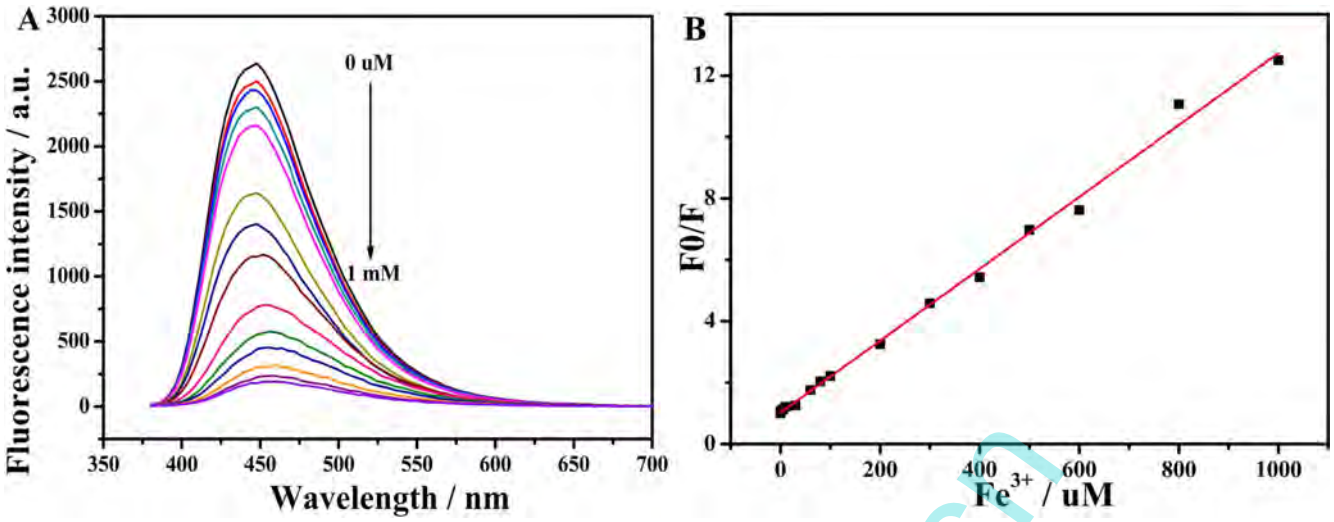

Figure 7. (A) Fluorescence spectra of the N-CQDs after treatment with different concentrations of Fe^{3+} (0–1000 μM) in the real sample. (B) Linear relationship between the F0/F and Fe^{3+} concentration.

promising candidate for practical applications of Fe^{3+} detection.

Detection of Fe^{3+} in real samples

In order to further investigate the as-prepared N-CQDs as a fluorescence probe to the detection of Fe(III) ion in a real environment, the performance of the N-CQDs for real sample analysis was studied. The fluorescence intensity of the N-CQDs with adding different concentrations of Fe(III) ions is displayed for real samples, as shown in figure 7(A). The data clearly show that the fluorescence intensity of the samples gradually declined as the concentration of Fe(III) ions increased. The standard curves for evaluating Fe(III) in the real lake water are displayed in figure 7(b). The results demonstrated that there was a good linear correlation in the range of 0–1000 μM with a correlation coefficient (R) of 0.99573. Although there were different kinds of mineral and organics in the real environment, the sensing system had a good detection for Fe(III) ion. The results revealed that the N-CQDs can be used as a sensor in real environmental samples.

Conclusion

In summary, a one-step method was successfully explored to synthesize N-CQDs using CA and EDA via a hydrothermal treatment. The results from various analyses indicated that the N-CQDs had a bright blue fluorescence, and displayed rapid response to the presence of Fe^{3+} ions. Meanwhile, there was a good linear relationship between the fluorescence intensity and concentration of Fe^{3+} ions within a wide concentration range between 0.5 and 1000 μM and the detection limit was estimated to be 79 nM in water. The obtained N-CQDs presented a good sensitive response to Fe^{3+} in real environmental samples.

Acknowledgments

This research was financially supported by the National Natural Science Foundation of China (51641303), the Priority Academic Program Development of Jiangsu Higher Education Institutions, the Natural Science Foundation of Jiangsu Province (BK20150155), the Fundamental Research Funds for the Central Universities (JUSRP51621A), the Department of Education in Anhui Province of China (2015LJRCTD001) and the Innovation Program for Graduate Education in Jiangsu Province (KYLX16_0794).

References

Atchudan R, Sethuraman M G and Yong R L 2016 Efficient synthesis of highly fluorescent nitrogen-doped carbon dots for cell imaging using unripe fruit extract of Prunus mume *Appl. Surf. Sci.* **384** 432–41

Chen Y, Wu Y, Weng B, Wang B and Li C 2015 Facile synthesis of nitrogen and sulfur co-doped carbon dots and application for Fe(III) ions detection and cell imaging *Sensors Actuators B* **223** 689–96

Ding H, Wei J S and Xiong H M 2014 Nitrogen and sulfur co-doped carbon dots with strong blue luminescence *Nanoscale* **6** 13817–23

Edison T N, Atchudan R, Sethuraman M G, Shim J J and Lee Y R 2016 Microwave assisted green synthesis of fluorescent N-doped carbon dots: cytotoxicity and bio-imaging applications *J. Photochem. Photobio.* B **161** 154–61

Fernando K A, Sahu S, Liu Y, Lewis W K, Guliants E A, Jafariyan A, Wang P, Bunker C E and Sun Y P 2015 Carbon quantum dots and applications in photocatalytic energy conversion *Acs Appl. Mater. Interf.* **7** 59–65

Fong J F Y, Chin S F and Ng S M 2016 A unique 'turn-on' fluorescence signalling strategy for highly specific detection of ascorbic acid using carbon dots as sensing probe *Biosens. Bioelectron.* **85** 844–52

Gong X, Lu W, Paau M C, Hu Q, Wu X, Shuang S, Dong C and Choi M M 2014 Facile synthesis of nitrogen-doped carbon dots for Fe(3+) sensing and cellular imaging *Anal. Chim. Acta* **861** 74–84

Han C, Wang R, Wang K, Xu H, Sui M, Li J and Xu K 2016 Highly fluorescent carbon dots as selective and sensitive 'on-off-on' probes for iron(III) ion and apoferritin detection and imaging in living cells *Biosens. Bioelectron.* **83** 229–36

Iqbal A, Tian Y, Wang X, Gong D, Guo Y, Iqbal K, Wang Z, Liu W and Qin W 2016 Carbon dots prepared by solid state method via citric acid and 1,10-phenanthroline for selective and sensing detection of Fe^{2+} and Fe^{3+} *Sensors Actuators B Chem.* **237** 408–15

Jian J and Chen W 2014 Synthesis of highly fluorescent nitrogen-doped graphene quantum dots for sensitive, label-free detection of Fe (III) in aqueous media *Biosens. Bioelectron.* **58C** 219–25

Jiang Y, Han Q, Jin C, Zhang J and Wang B 2015 A fluorescence turn-off chemosensor based on N-doped carbon quantum dots for detection of Fe^{3+} in aqueous solution *Mater. Lett.* **141** 366–8

Konstantatos G, Badioli M, Gaudreau L, Osmond J, Bernechea M, Fp G D A, Gatti F and Koppens F H 2012 Hybrid graphene-quantum dot phototransistors with ultrahigh gain *Nat. Nanotechnol.* **7** 363–8

Lai T, Zheng E, Chen L, Wang X, Kong L, You C, Ruan Y and Weng X 2013 Hybrid carbon source for producing nitrogen-doped polymer nanodots: one-pot hydrothermal synthesis, fluorescence enhancement and highly selective detection of Fe(III) *Nanoscale* **5** 8015–21

Li H, Kong W, Liu J, Liu N, Huang H, Liu Y and Kang Z 2015a Fluorescent N-doped carbon dots for both cellular imaging and highly-sensitive catechol detection *Carbon* **91** 66–75

Li L, Li L, Wang C, Liu K, Zhu R, Qiang H and Lin Y 2015b Synthesis of nitrogen-doped and amino acid-functionalized graphene quantum dots from glycine, and their application to the fluorometric determination of ferric ion *Microchim. Acta* **182** 763–70

Lim S Y, Shen W and Gao Z Q 2015 Carbon quantum dots and their applications *Chem. Soc. Rev.* **44** 362–81

Lin W, Long L, Yuan L, Cao Z and Feng J 2009 A novel ratiometric fluorescent Fe^{3+} sensor based on a phenanthroimidazole chromophore *Anal. Chim. Acta* **634** 262–6

Liu R, Wu D, Liu S, Koynov K, Knoll W and Li Q 2009 An aqueous route to multicolor photoluminescent carbon dots using silica spheres as carriers *Angew. Chem. Int. Edit.* **48** 4598–601

Lu W, Yong L, Li R, Shuang S, Dong C and Cai Z 2016 Facile synthesis of N-doped carbon dots as a new matrix for detection of hydroxy-polycyclic aromatic hydrocarbons by negative-ion matrix-assisted laser desorption/ionization time-of-flight mass spectrometry *Acs Appl. Mater. Interf.* **8** 12976–84

Mei Q, Jiang C, Guan G, Zhang K, Liu B, Liu R and Zhang Z 2012 Fluorescent graphene oxide logic gates for discrimination of iron (3+) and iron (2+) in living cells by imaging *Chem. Commun.* **48** 7468–70

Niu W J, Li Y, Zhu R H, Shan D, Fan Y R and Zhang X J 2015 Ethylenediamine-assisted hydrothermal synthesis of nitrogen-doped carbon quantum dots as fluorescent probes for sensitive biosensing and bioimaging *Sensors Actuators B Chem.* **218** 229–36

Ponomarenko L A, Schedin F, Katsnelson M I, Yang R, Hill E W, Novoselov K S and Geim A K 2008 Chaotic Dirac billiard in graphene quantum dots *Science* **320** 356–8

Qian Z, Ma J, Shan X, Feng H, Shao L and Chen J 2014 Highly luminescent N-doped carbon quantum dots as an effective multifunctional fluorescence sensing platform *Chem. Eur. J.* **20** 2254–63

Qu K, Wang J, Ren D J and Qu D X 2013 Carbon dots prepared by hydrothermal treatment of dopamine as an effective fluorescent sensing platform for the label-free detection of iron(III) ions and dopamine *Chem. Eur. J.* **19** 7243–9

Sheng Q Z, Yue S X, Jing C L, Rong C J and Feng H 2014 Dual-colored graphene quantum dots-labeled nanoprobes/graphene oxide: functional carbon materials for respective and simultaneous detection of DNA and thrombin *Nanotechnology* **25** 415501

Tan B, Zhao H, Du L, Gan X and Quan X 2016 A versatile fluorescent biosensor based on target-responsive graphene oxide hydrogel for antibiotic detection *Biosens. Bioelectron.* **83** 267–73

Wang L, Fernández-Terán R, Zhang L, Fernandes D L A, Tian L, Chen H and Tian H 2016 Organic polymer dots as photocatalysts for visible light-driven hydrogen generation *Angew. Chem. Int. Edit.* **55** 12306–10

Welsher K, Liu Z, Sherlock S P, Robinson J T, Chen Z, Dan D and Dai H 2009 A route to brightly fluorescent carbon nanotubes for near-infrared imaging in mice *Nat. Nanotechnol.* **4** 773–80

Wu Z L, Zhang P, Gao M X, Liu C F, Wang W, Leng F and Huang C Z 2013 One-pot hydrothermal synthesis of highly luminescent nitrogen-doped amphoteric carbon dots for bioimaging from Bombyx mori silk- natural proteins *J. Mater. Chem.* B **1** 2868–73

Xu H, Zhou S, Xiao L, Li S, Song T, Wang Y and Yuan Q 2015 Nanoreactor-confined synthesis and separation of yellow-luminescent graphene quantum dots with a recyclable SBA-15 template and their application for Fe(III) sensing *Carbon* **87** 215–25

Xu Q, Pu P, Zhao J, Dong C, Gao C, Chen Y, Chen J, Liu Y and Zhou H 2014 Preparation of highly photoluminescent sulfur-doped carbon dots for Fe(III) detection *J. Mater. Chem.* A **3** 542–6

Xu X, Ray R, Gu Y, Ploehn H J, Gearheart L, Raker K and Scrivens W A 2004 Electrophoretic analysis and purification of fluorescent single-walled carbon nanotube fragments *J. Am. Chem. Soc.* **126** 12736–7

Yang X, Zhuo Y, Zhu S, Luo Y, Feng Y and Dou Y 2014 Novel and green synthesis of high-fluorescent carbon dots originated from honey for sensing and imaging *Biosens. Bioelectron.* **60** 292–8

Yoon H *et al* 2016 Intrinsic photoluminescence emission from subdomained graphene quantum dots *Adv. Mater.* **28** 5255–61

Yu J 2015 Facilely synthesized N-doped carbon quantum dots with high fluorescent yield for sensing Fe^{3+} *New J. Chem.* **40** 2083–8

Yu J, Song N, Zhang Y K, Zhong S X, Wang A J and Chen J 2015 Green preparation of carbon dots by Jinhua bergamot for sensitive and selective fluorescent detection of Hg^{2+} and Fe^{3+} *Sensors Actuators B Chem.* **214** 29–35

Zhang H, Chen Y, Liang M, Xu L, Qi S, Chen H and Chen X 2014 Solid-phase synthesis of highly fluorescent nitrogen-doped carbon dots for sensitive and selective probing ferric ions in living cells *Anal. Chem.* **86** 9846–52

Zhang H, Zhang H, Aldalbahi A, Zuo X, Fan C and Mi X 2016 Fluorescent biosensors enabled by graphene and graphene oxide *Biosens. Bioelectron.* **89** (Pt 1) 96–106

Zhang R and Chen W 2014 Nitrogen-doped carbon quantum dots: facile synthesis and application as a 'turn-off' fluorescent probe for detection of Hg^{2+} ions *Biosens. Bioelectron.* **55** 83–90

Zhao H X, Liu L Q, Liu Z D, Wang Y, Zhao X J and Huang C Z 2011 Highly selective detection of phosphate in very complicated matrixes with an off-on fluorescent probe of europium-adjusted carbon dots *Chem. Commun.* **47** 2604–6

Zheng X T, Ananthanarayanan A, Luo K Q and Chen P 2015 Glowing graphene quantum dots and carbon dots: properties, syntheses, and biological applications *Small* **11** 1620–36

Zhou J, Han T, Ma H, Yan T, Pang X, Li Y and Wei Q 2015 A novel electrochemiluminescent immunosensor based on the quenching effect of aminated graphene on nitrogen-doped carbon quantum dots *Anal. Chim. Acta* **889** 82–9

Zhu S, Song Y, Zhao X, Shao J, Zhang J and Yang B 2015 The photoluminescence mechanism in carbon dots (graphene

quantum dots, carbon nanodots, and polymer dots): current state and future perspective *Nano Res.* **8** 355–81

Zuo P, Lu X, Sun Z, Guo Y and He H 2016 A review on syntheses, properties, characterization and bioanalytical applications of fluorescent carbon dots *Microchim. Acta* **183** 519–42